the high- (488 nm) or low-frequency (570 nm) side of the maximum. In addition, the relative intensities of these modes are very similar to those found for $Ru(bpy)_3^{2+}$. This further indicates the similarity of the excited-state geometries.

From the resonance Raman spectrum of $Ru(4,4'\text{-}Me_2bpy)_3^{2+}$ we note the small effect of symmetric (4,4') substitution on the frequencies of the resonance-enhanced Raman modes. Upon asymmetric substitution (i.e., one ring only), one observes the emergence of a pattern in which the Raman frequencies of one ring of the bipyridine system remain relatively unshifted as compared to those of the parent compound, whereas the substituted ring results in some shifted frequencies as well as additional resonance-enhanced bands due to mixing of substituent modes with resonance-enhanced ring modes. Of course, not all modes in the substituted-ring system are altered. In particular, the C–N stretching mode at about 1488 cm^{-1} seems quite invariant throughout the series of compounds with the exception of the 4,4'-dinitro compound. When such a dual set of observed modes exists, it gives rise to the possibility of following the transfer of charge onto the bipyridine ring system in the excited state as influenced by various substituents.

A comparison of the resonance Raman spectra for the parent compound and the ethoxy-substituted compound shows little change in the pattern of relative intensities even though new modes are observed due to the substitution. For the triethylphosphonium-substituted compound a very intense mode at 1534 cm^{-1} due to peripheral C–C stretch indicates the transfer of charge in the direction of the substituted ring system. The 1489-cm^{-1} band is equally intense but, along with the 1609-cm^{-1} mode, is apparently not sufficiently shifted from the unsubstituted ring value to allow a distinction. Note the low intensity of the 1570-cm^{-1} mode, which is assigned to the peripheral C–C stretch of the unsubstituted ring (corresponding to the 1534-cm^{-1} band).

In the nitro-substituted compound, the coupling of the strongly electron-withdrawing nitro group with the bipyridine π system has an even more dramatic effect on the resonance Raman spectrum. The dominance of the intense symmetric nitro stretching mode at 1359 cm^{-1} is unique among the spectra reported here and indicates that the nitro moiety is part of the chromophoric system. A great deal of charge must be transferred to the nitro group in the excited state, and this has been proposed[15] as an explanation for the unique absence of detectable luminescence for this substituted bipyridine complex of ruthenium(II). Because the nitro gorup can couple well with solvent (e.g., through hydrogen bonding), this may provide a facile, rapid pathway for vibrational depopulation of the excited state. The observed shift of only the nitro stretch to 1352 cm^{-1} in ethanol is further evidence of this type of solvent interaction.

As demonstrated by this study, the investigation of the resonance Raman spectra of an appropriate series of complexes of a metal with substituted ligands can provide insight concerning the nature of the electronic transitions for such a series. In addition, certain properties of the excited states may be inferred from such an analysis.

Acknowledgment. The authors wish to acknowledge support for this research provided by Research Corp., the Petroleum Research Fund, administered by the American Chemical Society, and the City University of New York PSC-BHE Research Award Program.

Registry No. $Ru(bpy)_3^{2+}$, 15158-62-0; $Ru(bpy)_2Cl_2$, 15746-57-3; $Ru(4,4'\text{-}Me_2bpy)_3^{2+}$, 32881-03-1; $Ru(4\text{-}OEtbpy)_3^{23}$, 80106-00-9; $Ru(4\text{-}PEt_3^+bpy)_3^{5+}$, 73891-49-3; $Ru(4\text{-}NO_2bpy)_3^{2+}$, 73891-47-1; $Ru(4,4'\text{-}(NO_2)_2bpy)_2Cl_2$, 73891-51-7; bpy, 366-18-7.

Contribution from the Department of Hydrocarbon Chemistry, Faculty of Engineering, Kyoto University, Kyoto 606, Japan

Electron Spin Resonance Study of Anion Radicals of Dicobalt Carbonyl Derivatives, $Co_2(CO)_6(ER_3)_2$ (ER_3 = P-*n*-Bu_3, $P(OMe)_3$, and As-*i*-Bu_3)

SHIGERU HAYASHIDA, TAKASHI KAWAMURA,* and TEIJIRO YONEZAWA

Received June 19, 1981

Anion radicals of $Co_2(CO)_6(ER_3)_2$ (ER_3 = P-*n*-Bu_3, $P(OMe)_3$, and As-*i*-Bu_3) are generated by exposure of 2-methyltetrahydrofuran solutions of their parent neutral complexes to ^{60}Co γ rays at 77 K and examined with ESR. The odd electron is accommodated in the intermetallic σ^* MO. The odd-electron densities on cobalt orbitals have small dependence on the axial ligand: $\rho(Co\ d_{z^2})$ = 0.31–0.32 and $\rho(Co\ 4s)$ = 0.010–0.015. The odd-electron density on the central atom of the axial ligand is 0.10 for the phosphine complex and 0.05–0.06 for the phosphite and the arsine complexes. This ligand dependence of the odd-electron distribution is interpreted with an orbital interaction scheme corresponding to a competitive sharing of the odd electron on the cobalt atoms between the lone pair orbitals on the axial and equatorial ligands. Carbonyl π^* and cobalt $4p_z$ orbitals are suggested to not be important contaminants in the intermetallic σ^* orbital. Anion radicals of dimanganese decacarbonyl derivatives are predicted to have a possibility of an axial ligand dependence of the odd-electron distribution different from that of the present dicobalt anions on a basis of an LCAO–Hartree–Fock–Slater calculation.

The cobalt complexes $Co_2(CO)_6(ER_3)_2$ (ER_3 = P-*n*-Bu_3, $P(OMe)_3$, and As-*i*-Bu_3) have a nonbridged D_{3d} geometry with an intermetallic single bond.[1] Manning[1a] suggested that the CoC stretching frequencies of this class of complexes correlate with π-acceptor properties of the axial ligands as in the case of dimanganese decacarbonyl derivatives.[2] Gray and his co-workers[3] have investigated their electronic spectra with conclusions that the intense absorptions at 393 and 360 nm of $Co_2(CO)_6(PPh_3)_2$ and $Co_2(CO)_6[P(OMe)_3]_2$, respectively, are due to the intermetallic σ–σ^* transition. Poe and Jackson[4]

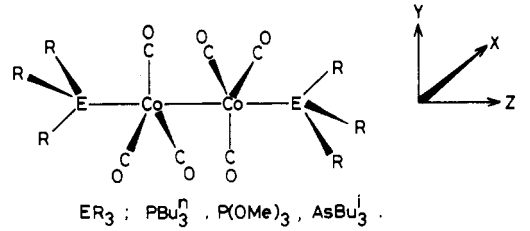

ER_3 ; PBu_3^n , $P(OMe)_3$, $AsBu_3^i$.

(1) (a) Manning, A. R. *J. Chem. Soc.* **1968**, 1135. (b) Ibers, J. A. *J. Organomet. Chem.* **1968**, *14*, 423.
(2) Lewis, J.; Manning, A. R.; Miller, J. R. *J. Chem. Soc.* **1966**, 845.
(3) Abrahamson, H. B.; Frazier, C. C.; Ginley, D. S.; Gray, H. B.; Lilienthal, J.; Tyler, D. R.; Wrighton, M. S. *Inorg. Chem.* **1977**, *16*, 1554.

0020-1669/82/1321-2235$01.25/0

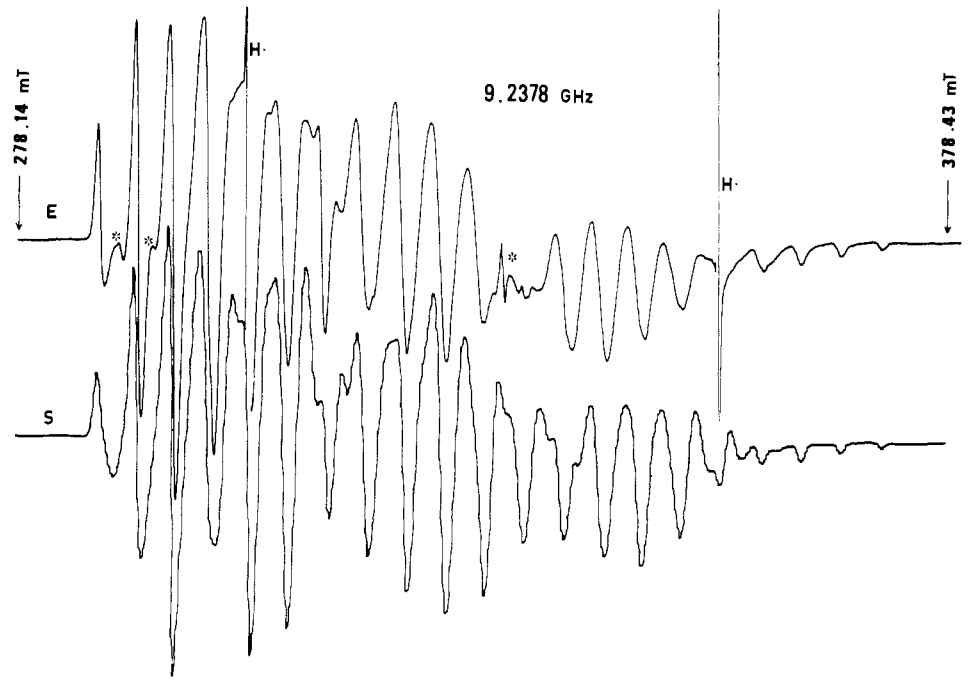

Figure 1. Experimental (E) and simulated (S) X-band ESR spectrum of $[Co_2(CO)_6[P(OMe)_3]_2]^-$ observed with microwave power of 0.5 mW at 77 K; signals with an asterisk are due to an unidentified species with short relaxation times and features with two asterisks in the $g \simeq 2.00$ region are due to unknown radicals with long relaxation times.

examined the axial ligand dependence of energies of this type of transitions and correlated them with ligands' σ basicities and π acidities.

In a preliminary paper[5] from this laboratory an ESR study of the anion radical of $Co_2(CO)_6(P\text{-}n\text{-}Bu_3)_2$ was reported with a conclusion that the odd electron is accommodated in the intermetallic σ^* MO and is delocalized rather extensively onto phosphorus lone pair orbitals. An odd-electron density on a ligand lone-pair orbital is a most direct measure of the σ donation from the ligand to the metal. In this report, the study is extended to anion radicals of $Co_2(CO)_6(ER_3)_2$ (ER_3 = $P(OMe)_3$ and As-*i*-Bu_3) to estimate the ligand dependence of metal–ligand σ interactions and resulting changes in the electronic structure of complexes.

Experimental Section

The dicobalt complexes were prepared by literature procedures.[1a] The solvent, 2-methyltetrahydrofuran (MTHF), was dried over a sodium–potassium alloy and transferred into a sample tube containing a small amount of a dicobalt complex on a vacuum line.

All the samples were irradiated at 77 K with a ^{60}Co source (0.041 Mrd/h) for periods between 20 and 60 h.

X-Band ESR spectra were recorded on a JEOL PE-2X spectrometer modified with a JEOL ES-SCXA gunn diode X-band microwave unit. The field sweep was monitored with proton NMR for each ESR measurement. A tunable NMR radio frequency was supplied from a JEOL ES-FC3 oscillator. ESR microwave and NMR radio frequencies were counted on a Takeda-Riken TR5501/TR5023 frequency counter. The spectrometer was operated under control of a JEOL EC-6 minicomputer, and the observed spectrum was digitized. The digitized spectrum was then submitted to a least-squares fitting to an axially symmetric spin Hamiltonian. Q-Band ESR spectra were observed on a JEOL FE-3Q spectrometer. When necessary, irradiated samples were annealed in a cold nitrogen gas flow controlled by a JEOL JES-VT-3A temperature controller. The sample was recooled to 77 K, and spectra were obtained at this temperature.

For analyses of ESR spectra of randomly oriented radicals with an axially symmetric spin Hamiltonian, a Fortran program, SAVE(AP) (system for analysis of various ESR spectra, axial symmetry, perturbation), was prepared by connecting a nonlinear optimization program, SALS (statistical analysis with least-squares fitting),[6] and a simulation program,[7] SIM(AP), based on a second-order perturbational solution[8] of the spin Hamiltonian.

Table I. ESR Parameters of $[Co_2(CO)_6(ER_3)_2]^-$

ER_3	$g_\parallel$	$g_\perp$	$10^4 \times \lvert A_\parallel(Co)\rvert$, cm^{-1}	$10^4 \times \lvert A_\perp(Co)\rvert$, cm^{-1}	$10^4 \times \lvert A_\parallel(E)\rvert$, cm^{-1}	$10^4 \times \lvert A_\perp(E)\rvert$, cm^{-1}
P-*n*-Bu_3	2.005_2	2.041_2	39.2	29.8	83.4	50.3
$P(OMe)_3$	2.005_7	2.041_4	39.1	31.6	120.8	110.6
As-*i*-Bu_3	2.006_6	2.057_5	45.7	19.6	96.6	85.3

Results

Irradiation of a frozen MTHF solution of $Co_2(CO)_6(P\text{-}n\text{-}Bu_3)_2$ at 77 K gave an axially symmetric paramagnetic species containing a pair of magnetically equivalent cobalt nuclei (^{59}Co, $I = {}^7/_2$, 100% natural abundance) and a pair of equivalent phosphorus nuclei (^{31}P, $I = {}^1/_2$, 100%). Its X-band ESR spectrum has been published elsewhere.[5] ESR parameters derived from a least-squares analysis are given in Table I. Its Q-band spectrum coincides well with the spectrum simulated with the same parameters.

The property of frozen MTHF as a suitable matrix for trapping of anionic species generated upon radiolysis by electron attachment to a solute[9] suggests that this radical is the anion of the complex. The validity of this electron-gain hypothesis was accomplished by a competitive electron capture between the dicobalt complex and *tert*-butyl bromide as described in the preliminary report.[5]

Figure 1a shows the low power (0.5 mW) X-band spectrum of a γ-irradiated MTHF glass containing $Co_2(CO)_6[P(OMe)_3]_2$ observed at 77 K after appropriate annealings. The microwave power dependence of the spectrum showed that there exist at least two paramagnetic species with different relaxation times. The low-power spectrum is mainly due to

(4) Poe, A. J.; Jackson, R. A. *Inorg. Chem.* **1978**, *17*, 2330.
(5) Hayashida, S.; Kawamura, T.; Yonezawa, T. *Chem. Lett.* **1980**, 517.
(6) Nakagawa, T.; Koyanagi, Y. "Manual for SALS"; Data Processing Center, University of Tokyo: Tokyo, Japan, 1979.
(7) Kawamura, T.; Fukamachi, K.; Sowa, T.; Hayashida, S.; Yonezawa, T. *J. Am. Chem. Soc.* **1981**, *103*, 364.
(8) Bleany, B. *Philos. Mag.* **1951**, *42*, 441.
(9) Hamill, W. H. "Radical Ions"; Kaiser, E. T., Kevan, L., Eds.; Wiley: New York, 1968; p 321.

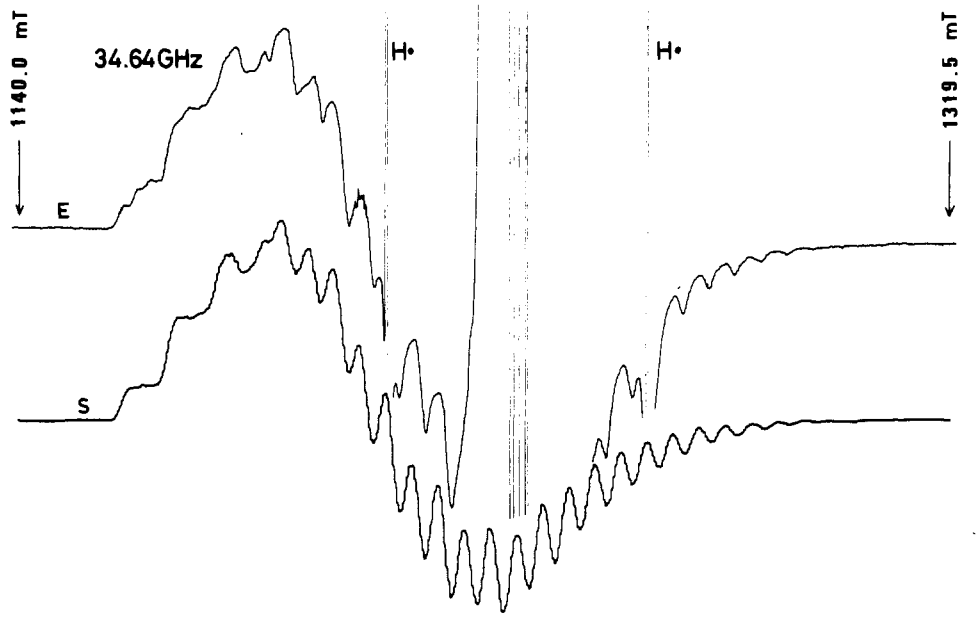

Figure 2. Experimental (E) and simulated (S) Q-band spectra of $[Co_2(CO)_6(As\text{-}i\text{-}Bu_3)_2]^{-\cdot}$ at 77 K. The intense absorptions in the central portion of the spectrum E are arising from solvent radicals.

a radical with an axially symmetric spin Hamiltonian and with a long relaxation time. The radical has pairs of magnetically equivalent cobalt and phosphorus nuclei. The experimental spectrum was reproduced with ESR parameters listed in Table I. Its Q-band experimental spectrum also coincides well with the reproduced one with the same parameter set. By analogy with the case for $Co_2(CO)_6(P\text{-}n\text{-}Bu_3)_2$ the radical giving the spectrum in Figure 1 is attributed to the parent anion, $[Co_2(CO)_6[P(OMe)_3]_2]^{-\cdot}$. High-power (100–200 mW) X-band spectra were too complicated to be analyzed.

Exposure of $Co_2(CO)_6(As\text{-}i\text{-}Bu_3)_2$ in MTHF to γ rays at 77 K produced a thermally unstable radical that decomposes quickly during trial annealings to remove solvent radicals. The irradiated samples of the arsine complex were examined without annealings. The X-band ESR spectrum due to the paramagnetic species from the arsine complex was poorly defined because of overlap with solvent radical features. Its Q-band spectrum (Figure 2) was examined to diminish this complexity. The spectrum was analyzed as originating from an axially symmetric species containing two equivalent cobalt nuclei and two equivalent arsenic nuclei (^{75}As, $I = {}^3/_2$, 100%). The analysis of the spectrum is listed in Table I. The comparison between the experimental and the simulated X-band spectra has also confirmed the present analysis, although the former is overlapped seriously with signals due to solvent radicals. This radical is assigned to $[Co_2(CO)_6(As\text{-}i\text{-}Bu_3)_2]^{-\cdot}$.

Discussion

Symmetry of Odd-Electron Orbital. Since ESR spectra of the present three anions fit axially symmetric spin Hamiltonians with hyperfine splitting tensors of a pair of equivalent cobalt nuclei and a pair of equivalent axial ligand nuclei (E), it is reasonable to assume that the anions have D_{3d} geometries as in the case of their parent neutral complexes. The parallel axis of the present axially symmetric spin Hamiltonian should coincide with the molecular z axis, the C_3 axis of the D_{3d} geometry, otherwise the parallel axis of the axially symmetric g tensor and those of the hyperfine splitting tensors cannot be parallel to each other.

The cobalt hyperfine splitting tensor of $[Co_2(CO)_6(As\text{-}i\text{-}Bu_3)_2]^{-\cdot}$ was separated into approximate Fermi contact and spin–dipolar splitting terms by ignoring the second-order effects[7] of unquenched orbital angular momenta of electrons. The dipolar splitting term is assumed to be arising from an odd-electron density on a cobalt 3d atomic orbital (AO). The experimental anisotropic term is too large to attribute it to an odd-electron density on a cobalt 4p AO that is diffuse and has a too small expectation value of r^{-3}. Then we can correlate an odd-electron density on a cobalt 3d AO and the experimental cobalt splitting tensor as in

$$A_{\parallel}(\mathrm{Co}) = a'(\mathrm{Co}) + 2B(\mathrm{Co\ d})\,\rho'(\mathrm{Co\ d}) \quad (1)$$

$$A_{\perp}(\mathrm{Co}) = a'(\mathrm{Co}) - B(\mathrm{Co\ d})\,\rho'(\mathrm{Co\ d}) \quad (2)$$

where the prime on a(Co), the Fermi contact term for the cobalt nucleus, and that on ρ(Co d), an odd-electron density on a cobalt 3d AO, are to indicate that these are obtained by ignoring the second-order effects of unquenched orbital angular momenta of electrons, and $2B$(Co d) is an anisotropic splitting constant of a cobalt nucleus with an unit 3d odd-electron density which has been calculated by Morton and Preston.[10]

If a negative sign were assigned to $A_{\parallel}$(Co) (the second and the fourth data rows in Table II), the odd electron would be concluded to be accommodated in a molecular orbital (MO) consisting of cobalt d_{xy} or $d_{x^2-y^2}$ AO's. In a D_{3d} geometry, this MO belongs to a degenerate e_g or e_u symmetry. The spectrum has too narrow line widths to attribute it to a species with an orbitally degenerate ground state. The anion radical may have been deformed slightly from the D_{3d} geometry in frozen matrices, and the odd electron occupies the MO containing a d_{xy} (or $d_{x^2-y^2}$) AO of a cobalt atom. In this case, the MO, containing the $d_{x^2-y^2}$ (or d_{xy}) AO of the cobalt atom and having been degenerate with the odd-electron orbital in the original

Table II Possible Sign Combinations for Cobalt Splittings of $[Co_2(CO)_6(As\text{-}i\text{-}Bu_3)_2]^{-\cdot}$ and Approximate Odd-Electron Distributions[a]

sign of $A_{\parallel}$(Co)	sign of $A_{\perp}$(Co)	$10^4 a'$(Co), cm^{-1}	$10^4 \times 2B$(Co d) $\times \rho'$(Co d), cm^{-1}	ρ'(Co d)
+	−	2.2	43.5	0.27 (d_{z^2})
−	+	−2.2	−43.5	0.27 (d_{xy} or $d_{x^2-y^2}$)
+	+	28.3	17.4	0.11 (d_{z^2})
−	−	−28.3	−17.4	0.11 (d_{xy} or $d_{x^2-y^2}$)

[a] Analysis according to eq 1 and 2.

(10) Morton, J. R.; Preston, K. F. *J. Magn. Reson.* **1978**, *30*, 577.

Table III Odd-Electron Distribution in $[Co_2(CO)_6(ER_3)_2]^{-}$.[a]

ER_3	ρ(Co s)	ρ(Co d_{z^2})	ρ(E s)	ρ(E p_z)
P-*n*-Bu_3	0.009–0.015	0.31_3	0.014	0.09
$P(OMe)_3$	0.009–0.015	0.32_0	0.026	0.02_9
As-*i*-Bu_3	0.010–0.016	0.31_0	0.018	0.03_4

[a] Analysis according to eq 3–7.

D_{3d} geometry, is vacant and should induce a large negative shift of $g_\parallel$ from the free spin value, $g_e = 2.0023$.[11] This is contrary to the experimental results. Thus we can conclude that the odd electron occupies a MO consisting of cobalt d_{z^2} AO's (the first and the third data rows of Table II). This odd-electron orbital belongs to a_{1g} or a_{2u} symmetry. In this model $g_\parallel$ is expected to be close to g_e.[11] This is consistent with the experimental results, although the observed values of $g_\parallel$ have a trend of a small positive shift from g_e.[12] This is due to spin polarization.[13]

Energies for intermetallic σ–σ^* transitions of the present type of neutral dicobalt complexes are rather small.[3,4] Reduction of neutral complexes with sodium amalgum induces fission of the intermetallic σ bond.[14] These indicate that the intermetallic σ^* MO is a low-lying vacant orbital of the present type of complexes. Since the foregoing analysis of ESR results has shown that the odd-electron orbital of the anion radical has cobalt d_{z^2} AO's as its constituents, it can be assigned to the a_{2u} intermetallic σ^* MO. The choice of a negative sign for $A_\perp$(Co) (the first data row of Table II) results in the estimation of ρ'(Co d_{z^2}) = 0.27, which is more consistent with the assignment than the other choice of the sign (the third data row of Table II). On the basis of similar analyses, the odd-electron orbitals of $[Co_2(CO)_6(P\text{-}n\text{-}Bu_3)_2]^{-}\cdot$ and $[Co_2(CO)_6[P(OMe)_3]_2]^{-}\cdot$ are assigned to their intermetallic σ^* MO's and signs of their $A_\parallel$(Co) and $A_\perp$(Co) are chosen as positive and negative, respectively. These results are parallel to the study of anion radicals of dimanganese decacarbonyl and dirhenium decacarbonyl reported by Bratt and Symons,[15] in which the odd electron has been shown to be accommodated in the intermetallic σ^* MO.

The a_{2u} intermetallic σ^* odd-electron orbital, whose major constituent is the antiphase combination of the d_{z^2} AO's, can formally contain lone-pair orbitals on the axial and equatorial ligands in antibonding phase and the π^* orbitals of the equatorial carbonyls[16] in bonding phase. Cobalt 4s and $4p_z$ AO's would be also mixed more or less in the odd-electron orbital.

Odd-Electron Distribution. Orbital angular momenta of electrons in the present radicals are not quenched completely as evident from appreciable shifts of some principal values of **g** tensors from g_e. Further refinements of analyses of the odd-electron distribution require corrections for the second-order terms in hyperfine splitting tensors originating from the unquenched momenta.[7]

With the assumption that the l–s coupling of the odd electron takes place only in Co 3d AO's and that there is only small mixing between Co 3d AO's and ligand orbitals in e_u MO's, the odd-electron distributions in the present species can be correlated with the principal values of their splitting tensors as follows:

$$A_\parallel(\text{Co}) = a(\text{Co}) + 2B(\text{Co } d_{z^2})\,\rho(\text{Co } d_{z^2}) - {}^1/_4B(\text{Co } d_{z^2})\,\Delta g_\perp \quad (3)$$

$$A_\perp(\text{Co}) = a(\text{Co}) - B(\text{Co } d_{z^2})\,\rho(\text{Co } d_{z^2}) + {}^{15}/_8B(\text{Co } d_{z^2})\,\Delta g_\perp \quad (4)$$

$$A_\parallel(\text{E}) = Q_V(\text{E})\,\rho(\text{E s}) + 2B(\text{E } p_z)\,\rho(\text{E } p_z) \quad (5)$$

$$A_\perp(\text{E}) = Q_V(\text{E})\,\rho(\text{E s}) - B(\text{E } p_z)\,\rho(\text{E } p_z) \quad (6)$$

where $\Delta g_\perp$ is the shift of $g_\perp$ from g_e, $2B(\text{A }\chi)$ designates a parallel component of a dipolar hyperfine splitting of a nucleus, A, with an unit odd-electron density of its valence shell AO, χ, $\rho(\text{A }\chi)$ shows the odd-electron density on this AO, and Q_V(A) notes a Fermi contact term due to a nucleus, A, with an unit odd-electron density on its valence shell s AO. Values of $2B(\text{A }\chi)$ and Q_V(A) have been calculated by Morton and Preston.[10] With the assumption that the contribution of the inner-shell spin polarization to the Fermi contact term of the cobalt splitting is proportional to ρ(Co d_{z^2}), ρ(Co s) can be evaluated from a(Co) as:

$$a(\text{Co}) = Q_I(\text{Co})\,\rho(\text{Co } d_{z^2}) + Q_V(\text{Co})\,\rho(\text{Co s}) \quad (7)$$

where Q_I(Co) is the inner-shell spin polarization coefficient which has been estimated as $(-94 \text{ to } -131) \times 10^{-4}$ cm^{-1}.[17]

The odd electron of the present anions is expected to be delocalized onto valence-shell s and p_z AO's on the axial ligand atom E, resulting in positive spin densities on both of these AO's. This expectation is satisfied only when we assume positive signs for both of $A_\parallel$(E) and $A_\perp$(E). Odd-electron densities on valence-shell AO's of the atom E are estimated by neglecting inner-shell spin polarization. Thus estimated odd-electron distributions are given in Table III.

The experimental anisotropy of the cobalt hyperfine splitting cannot be separated into the contribution from odd-electron density on the d_{z^2} AO and that on the cobalt $4p_z$ AO. As mentioned before, however, the latter has only small effect on the cobalt splitting. Thus the present neglect of the anisotropy due to the $4p_z$ odd-electron density should not have induced appreciable errors in the estimation of that on the d_{z^2} AO.

Ligand Dependence of Odd-Electron Distribution. The odd-electron densities on the axial ligand in the phosphite and the arsine complexes are considerably smaller than that in the phosphine complex. Since the ionization potential of trimethyl phosphite is 1 eV greater than that of tri-*n*-butylphosphine,[18] a less effective odd-electron delocalization from the cobalt d_{z^2} AO's onto the phosphorus lone-pair orbitals is reasonable for the phosphite complex in comparison to that for the phosphine complex. The difference in the odd-electron distribution between the phosphine and the arsine complexes seems to be due to less efficient overlap between the cobalt d_{z^2} orbital and the axial ligand lone-pair orbital for the arsine complex in comparison with that involved in the phosphine complex, since the ionization potentials of both axial ligands are expected to be similar in analogy to those of PPh_3 and $AsPh_3$.[19]

As seen in Table III, the odd-electron density on the cobalt atom remains approximately constant for all of these complexes, although the odd-electron density on the axial ligand has an appreciable ligand dependence. This indicates an existence of a reservoir orbital(s) which competes with the lone

(11) For the theory of **g** tensor, see: Stone, A. J. *Proc. R. Soc. London, Ser. A* **1963**, *271*, 424.
(12) Once we reported the $g_\parallel$ of $[Co_2(CO)_6(P\text{-}n\text{-}Bu_3)_2]^{-}\cdot$ to be 2.0094,[5] but the present refinement of analysis of the spectra by least-square fittings has led to $g_\parallel = 2.0052$.
(13) Kawamura, T.; Hayashida, S.; Yonezawa, T. *Chem. Phys. Lett.* **1981**, *77*, 348.
(14) Hieber, W.; Kruck, T. *Z. Naturforsch., B: Anorg. Chem., Org. Chem., Biochem., Biophys., Biol.* **1961**, *16B*, 709.
(15) Bratt, S. W.; Symons, M. C. R. *J. Chem. Soc. Dalton Trans.* **1977**, 1314.
(16) (a) A large mixing of π^* orbitals of equatorial carbonyls in both of intermetallic σ and σ^* MO's of dimanganese decacarbonyl has been found in MO calculations.[10b,c] (b) Elian, M.; Hoffmann, R. *Inorg. Chem.* **1975**, *14*, 1058. (c) Heijser, W.; Baerends, E. J.; Ros, P. *Symp. Faraday Soc.* **1980**, *14*, 211.
(17) (a) Anderson, O. P.; Fieldhouse, S. A.; Forbes, C. E.; Symons, M. C. R. *J. Organomet. Chem.* **1976**, *110*, 247. (b) Peake, B. M.; Rieger, P. H.; Robinson, B. H.; Simpson, J. *J. Am. Chem. Soc.* **1980**, *102*, 156.
(18) Distefano, G.; Innorta, G.; Pignatora, S.; Foffani, A. *J. Organomet. Chem.* **1968**, *14*, 165.
(19) Preer, J. R.; Tsay, F. D.; Gray, H. B. *J. Am. Chem. Soc.* **1972**, *94*, 1875.

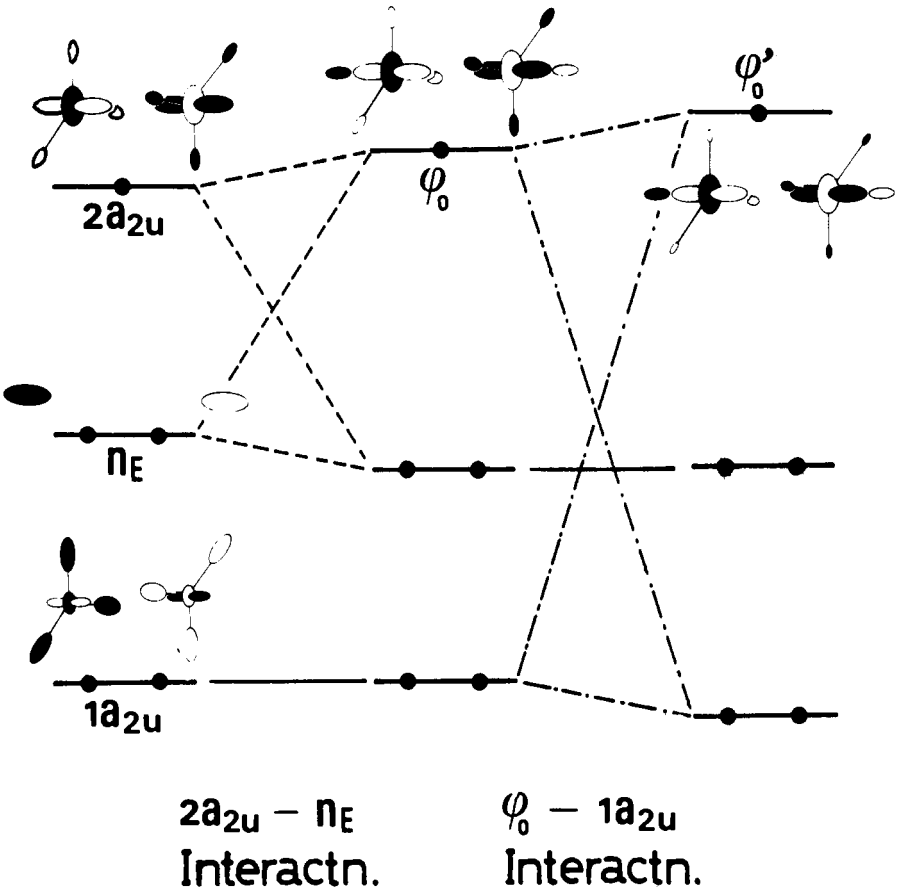

Figure 3. Orbital interactions among cobalt d_{z^2} and lone-pair orbitals on axial and equatorial ligands.

pair orbitals on the axial ligands for the share of the odd electron. Candidates for such a reservoir are a_{2u} symmetry orbitals of cobalt $4p_z$ AO's, carbon lone pair, and π^* orbitals on equatorial carbonyls.

First, we examine the axial ligand dependence of the weight of the mixing of the carbon lone-pair orbitals into the intermetallic σ^* MO. In a hypothetical anion radical in which cobalt d_{z^2} AO's are allowed to interact with the lone-pair orbitals of carbonyls but forbidden to interact with those of axial ligands, the odd-electron orbital ($2a_{2u}$ in Figure 3) is the antibonding combination of the d_{z^2} AO's with an antiphase contaminant of the a_{2u} combination of the carbonyl lone-pair orbitals. Correspondingly, the lone-pair orbital of the equatorial carbonyls ($1a_{2u}$) has the d_{z^2} orbital as a contaminant in a bonding phase. When the interaction between cobalt d_{z^2} AO's and lone-pair orbitals of axial ligands (the a_{2u} axial ligand lone-pair orbital is designated as n_E in Figure 3) is taken into account, the n_E orbital mixes into the $2a_{2u}$ odd-electron orbital in an antiphase manner to form a delocalized odd-electron orbital, ψ_O. The equatorial carbonyl lone-pair orbital, $1a_{2u}$, can now mix into ψ_O through the overlap between the d_{z^2} component in $1a_{2u}$ and the n_E component in ψ_O. The phase relation among the interacting orbitals indicates that the weight of the carbonyl lone-pair orbitals in the final odd-electron orbital, ψ_O', decreases as the mixing of n_E into the $2a_{2u}$ orbital increases. This is a reflection of a competitive σ donation to the metal from axial and equatorial ligands. Lone-pair orbitals on equatorial carbonyls can thus compete with those on axial ligands in the sharing of the odd electron on the cobalt atoms.

Second, we examine the ligand dependence of the odd-electron distribution expected for the case in which there exists an appreciable odd-electron delocalization onto the carbonyl π^* orbitals. As in the foregoing analysis, the a_{2u} symmetry orbitals of cobalt d_{z^2} and of carbonyl π^* orbitals interact with each other in the first step. The resulting orbital of the intermetallic σ^* character and that with the carbonyl π^* character are designated as $2a_{2u}$ and $3a_{2u}$, respectively, in Figure 4. The interaction between axial ligand lone-pair and cobalt d_{z^2} orbitals mixes the a_{2u} combination of the former orbitals, n_E, into the $2a_{2u}$ orbital, resulting in a delocalized odd-electron orbital, ψ_O. The interaction between the n_E component in ψ_O and the d_{z^2} component in $3a_{2u}$ induces a mixing of $3a_{2u}$ into ψ_O in an in-phase manner with respect to the interacting region, resulting in the final odd-electron orbital, ψ_O'. The phase relation among the interacting orbitals leads to a prediction that the increase of the odd-electron density on the axial ligand should be accompanied with the increase of that on the carbonyl π^* orbitals. This is a reflection of one of mechanisms for the increase of the π back-donation toward the equatorial carbonyls induced by the increase of the σ donation from the axial ligands. The carbonyl π^* orbitals cannot behave as the reservoir orbital to make the odd-electron density on the cobalt atom insensitive to the axial ligand.

Third, we examine the axial ligand dependence of the odd-electron density on a cobalt $4p_z$ AO expected for a model where the odd-electron density on this AO is appreciable. The prediction of the dependence depends upon relative magnitudes of interactions of a $4p_z$ AO on a cobalt atom with the d_{z^2} AO on the neighboring cobalt atom and with the lone-pair orbital on the neighboring axial ligand. Since the overlap integral between the cobalt $4p_z$ and the phosphorus $3p_z$ AO's is 0.339[20] and is larger than that between the former AO and the d_{z^2} AO which is 0.112,[20] the $4p_z$ AO is expected to interact more strongly with the axial ligand lone-pair orbital than with the

(20) (a) Calculated for the geometry of $Co_2(CO)_6(P\text{-}n\text{-}Bu_3)_2$[1b] with STO-6G basis sets[20b] with scale factors given by Clementi.[20c] The scale factor of the cobalt 4p AO was approximated with that for the cobalt 4s AO. (b) Stewart, R. F. *J. Chem. Phys.* **1970**, *52*, 431. (c) Clementi, E.; Roetti, C. *At. Data Nucl. Data Tables* **1974**, *14*, 177.

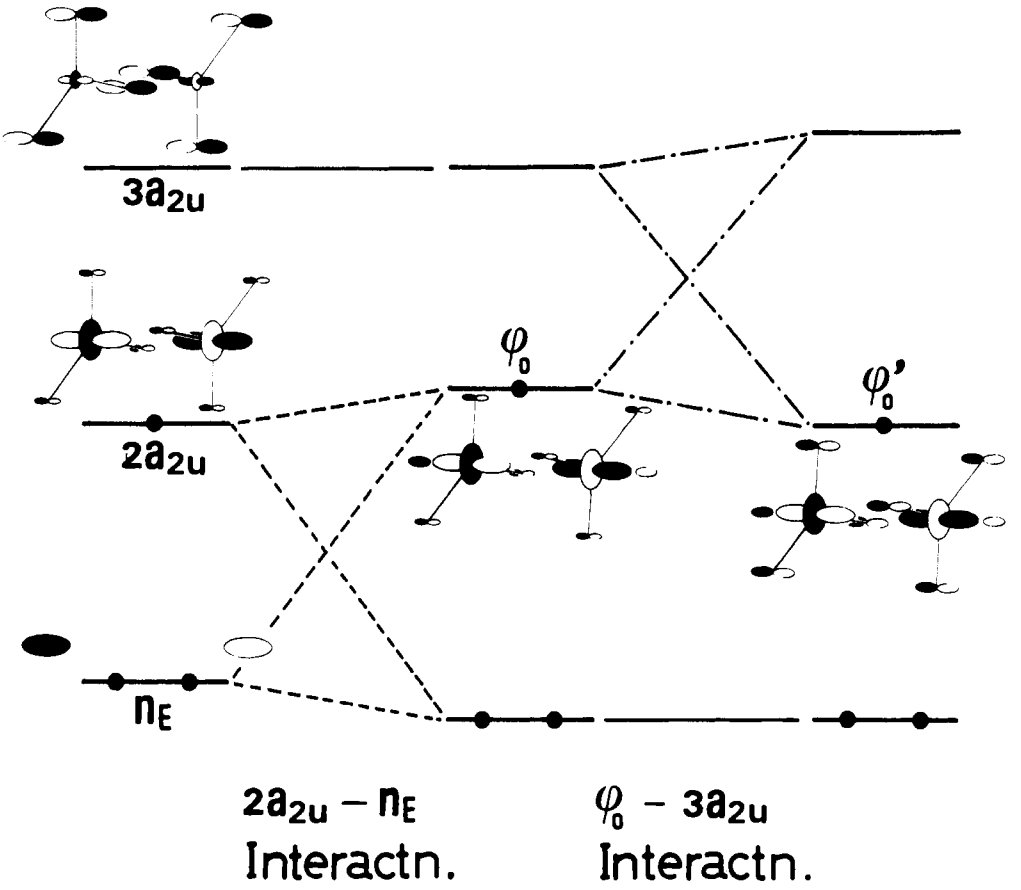

Figure 4. Orbital interactions among cobalt d_{z^2}, carbonyl π^*, and lone-pair orbitals on axial ligands. Only the carbon 2p AO's of carbonyl π^* orbitals are shown.

d_{z^2} AO. Thus the $4p_z$ AO would mix into the odd-electron orbital, resulting in a pd hybridization on the cobalt atom, as to diminish its antibonding destabilization between the cobalt atom and the axial ligand rather than to shift the odd electron away from the intermetallic region. When the odd-electron density on the axial ligand increases as a result of an increase of its σ basicity, the weight of the $4p_z$ AO in the odd-electron orbital is expected to increase for a further diminution of the metal–ligand antibonding character. The odd-electron density on the cobalt $4p_z$ AO is thus expected to increase when that on the axial ligand increases. The cobalt $4p_z$ AO may not behave as a reservoir orbital to make the odd-electron density on the cobalt atom independent from the axial ligand.

On the basis of the foregoing arguments, we propose that the intermetallic σ^* MO of the present type of dicobalt carbonyl complexes, constructed mainly from the cobalt $3d_{z^2}$ AO's (64%), contains the lone-pair orbitals on the axial ligands (10–20%) together with those on the equatorial carbonyls and that these lone-pair orbitals compete with each other for the share of the odd electron on the cobalt atoms.

The LCAO–Hartree–Fock–Slater calculation of dimanganese decacarbonyl[16c] has shown that its intermetallic σ^* MO is constructed mainly from the manganese $3d_{z^2}$ AO's (41%) and the π^* orbitals of the equatorial carbonyls (37%). The relative importance of the carbon lone-pair orbitals and of the π^* orbitals on the equatorial carbonyls for the intermetallic σ^* MO differs between the dimanganese complex and the present type of dicobalt complexes. We expect that the axial ligand dependence of the odd-electron distribution in anion radicals of derivatives of the dimanganese complex would be different from that observed for the present dicobalt anions. In the former anions, an enhanced decrease of the odd-electron density on the metal atom is expected to accompany an increase of that on the axial ligand, if the ligand dependence arises from the change of its σ basicity and if the MO calculation is reliable.

Acknowledgment. We are grateful to Messrs. M. Kohno, K. Deguchi, and K. Fujii (JEOL) for the facilities used to measure Q-band ESR spectra. Samples were exposed to γ rays at the Research Laboratory of Radioisotopes of Kyoto University. Nonlinear optimization analyses of ESR spectra were performed on a FACOM M200 computer at the Data Processing Center of Kyoto University.

Registry No. $[Co_2(CO)_6(P\text{-}n\text{-}Bu_3)_2]^{-\cdot}$, 74191-99-4; $[Co_2(CO)_6[P(OMe)_3]_2]^{-\cdot}$, 81205-55-2; $[Co_2(CO)_6(As\text{-}i\text{-}Bu_3)_2]^{-\cdot}$, 81205-56-3.

Supplementary Material Available: Figures of experimental and simulated X-band and Q-band spectra of $[Co(CO)_3(P\text{-}n\text{-}Bu_3)_2]^{-\cdot}$, $[Co_2(CO)_6[P(OMe)_3]_2]^{-\cdot}$, and $[Co(CO)_3(As\text{-}i\text{-}Bu_3)_2]^{-\cdot}$ (4 pages). Ordering information is given on any current masthead page.